

Correlation of diffusion tensor imaging parameters and Gleason scores of prostate cancer

WEIZHONG TIAN¹, JI ZHANG¹, FANGZHENG TIAN¹,
JUNKANG SHEN², TIANLI NIU³, GUOHUA HE⁴ and HONG YU⁵

¹Department of Radiology, Taizhou People's Hospital, Taizhou, Jiangsu 225300; ²Department of Radiology, The Second Affiliated Hospital of Soochow University, Suzhou, Jiangsu 215004; ³Department of Urinary Surgery, Taizhou People's Hospital; ⁴Department of Urinary Surgery, Taizhou Hospital of Traditional Chinese Medicine; ⁵Department of Pathology, Taizhou People's Hospital, Taizhou, Jiangsu 225300, P.R. China

Received June 17, 2016; Accepted April 10, 2017

DOI: 10.3892/etm.2017.5363

Abstract. The aim of the present study was to explore the association between the parameters of diffusion tensor imaging (DTI), including fractional anisotropy (FA) values, apparent diffusion coefficient (ADC) values and the diffusion tensor tractography (DTT) map, with the Gleason score of prostate cancer (PCa). A retrospective study of 50 cases of PCa confirmed by biopsy or surgical pathology was performed. Conventional magnetic resonance imaging and DTI scans were conducted in these cases. The 50 cases of PCa were divided into three groups, including low, intermediate and high grade, according to the Gleason score. Post-DTI processing was performed using Neuro 3D software, in order to measure the FA and ADC values, and map the prostate fibers. Differences in FA and ADC values among the various PCa groups were examined using analysis of variance, while the correlation of FA and ADC values with the Gleason score was studied using Pearson correlation analysis. The obtained DTT map clearly demonstrated the spatial structure of the prostate fibers. The fibers of the cancer area were dense without interruption in the low-grade group, sparse and disordered in the intermediate-grade group, and were disordered, sparse or even absent in the high-grade group. The FA values were 0.284 ± 0.313 , 0.293 ± 0.347 and 0.369 ± 0.347 , respectively, with statistically significant differences observed among the three groups ($F=234.533$; $P<0.05$) and between each group ($P<0.05$). In addition, the FA value of PCa was positively correlated with the Gleason score ($r=0.884$; $P<0.05$). The ADC values of the low-, intermediate- and high-grade groups were

$1.070 \pm 0.072 \times 10^{-3}$, $0.961 \pm 0.081 \times 10^{-3}$ and $0.821 \pm 0.048 \times 10^{-3}$, respectively, which demonstrated statistically significant differences among the three groups ($F=49.987$; $P<0.05$) and between each group ($P<0.05$). Furthermore, the ADC values of PCa were negatively correlated with Gleason score ($r=-0.810$; $P<0.05$). In conclusion, there was an association between DTI parameters and Gleason score, which may be used to evaluate the grading and prognosis of PCa.

Introduction

Prostate cancer (PCa) is one of the most common types of cancer and the second leading cause of cancer related mortality in males in the United States (1). The incidence of PCa in China is increasing due to the ageing population and western culture (2).

Current PCa screening tools used, include the detection of increased levels of serum prostate specific antigen and digital rectal examination, however, the two methods are limited in accuracy in diagnosing PCa and the evaluation of aggressiveness (3). To date, the most effective technique for localizing and staging prostate cancer is magnetic resonance imaging (MRI). MRI provides excellent high-contrast and high-resolution morphological images of the human prostate (3). The guidelines for routine diagnosis and treatment of prostate disease outlined by the European Society of Urogenital Radiology currently recommend examination by prostate multi-parametric MRI, including the uses of T1-weighted imaging (T1WI), T2-weighted imaging (T2WI) and diffusion-weighted imaging (DWI) (4,5). Preoperative evaluation of PCa aggressiveness is a prerequisite to offer personalized treatment options. The Gleason score acquired from biopsy or surgery on the prostate is important for the evaluation of PCa aggressiveness, selection of clinical treatment options and assessment of prognosis (6). Several studies have investigated the correlation between the apparent diffusion coefficient (ADC) value obtained from the DWI sequence and Gleason score noninvasively, however a consensus is yet to be reached on this (7-9).

Diffusion tensor imaging (DTI) is a novel and promising technique with wide clinical applications, especially in

Correspondence to: Dr Ji Zhang, Department of Radiology, Taizhou People's Hospital, 210 Yinchun Road, Taizhou, Jiangsu 225300, P.R. China
E-mail: xujw634@126.com

Key words: prostate cancer, diffusion tensor imaging, diffusion tensor tractography, apparent diffusion coefficient, fractional anisotropy, magnetic resonance imaging, Gleason score

neuro-and musculoskeletal imaging. DTI can provide ADC and fractional anisotropy (FA) values and diffusion tensor tractography (DTT), which may reflect physiological features and pathological changes at microscopic level (10). The clinical application of DTI of the prostate has been confirmed by several studies (11,12).

The present study aimed to explore the correlation of ADC and FA values, and DTT, with the Gleason score for the prediction of PCa pathological grading, in order to improve selection of an appropriate treatment and assessment of patient prognosis.

Materials and methods

Clinical data. A retrospective analysis of 50 patients with PCa, diagnosed by biopsy or surgical pathology diagnosis between June 2013 and December 2015 at Taizhou People's Hospital (Taizhou, China) was conducted. Patients were 43-88 years old (72.8 ± 7.98 years), with 1.74-169.35 ng/ml prostate-specific antigen (normal reference range, 0-4 ng/ml). The symptoms of these patients included dysuria, hematuria and hematospermia. The inclusion criteria for patients in the current study were as follows: i) Conventional MRI and DTI scanning was performed without puncture, cryotherapy, radiotherapy and chemotherapy or endocrine therapy; and ii) transrectal ultrasound guide biopsy or surgical resection was conducted within 2 weeks of MRI examination. Written informed consent was obtained from all participants prior to the investigation.

Inspection methods. At 1 day before examination, low residue diet and oral laxatives were administered in the evening in order to clean the intestinal track and allow for adequate bladder filling. Axis T1WI, T2WI-fat suppression (FS) and DTI scans regarding the prostate were performed using a 3.0 T MRI scanner (Siemens AG, Munich, Germany) with 8-channel phased array coil.

The axial T1WI scanning parameters were as follows: Repetition time (TR), 140 msec; echo time (TE), 2.46 msec; field of view (FOV), 230x230 mm; matrix, 288x320; layer thickness, 3.0 mm; no spacing; number of layers, 20; flip angle, 70°; acquisition time, 29 sec. The axial T2WI-FS scanning parameters were as follows: TR, 3540 msec; TE, 124 msec; FOV, 230x230 mm; matrix, 230x288; layer thickness, 3.0 mm; no spacing; number of layers, 20; flip angle, 150°; signal-to-noise ratio (SNR), 1; averages, 3; acquisition time, 177 sec.

DTI was performed with a single-shot EPI technique using the following parameters: TR, 3,000 msec; TE, 93 msec; FOV, 230x230 mm; matrix, 230x128 mm; slice thickness, 3.0 mm; no spacing, number of layers, 20. The diffusion gradients were applied in 12 directions with two b values of 0 and 800 s/mm². The acquisition time of DTI was approximately 4 min 5 sec. Axial T2WI-FS images were used as anatomical and morphological orientation for DTI analysis.

Data analysis and image processing. Following data acquisition, all of the images were transmitted to the digital workstation [Syngo MultiModality Workplace (SMMW); Siemens AG, Munich, Germany]. The DWI map is auto obtained following scanning. The calculation of the FA and ADC values and DTT

image processing were performed using Neuro 3D software included in the SMMW. The region of interest (ROI) was drawn in the area of PCa on T2WI-FS confirmed by biopsy or surgery. The ROIs on T2WI-FS were automatically transferred onto the co-registered FA and ADC maps constructed from DTI. Two radiologists with extensive experience in MRI diagnosis drew all of the ROIs. While drawing ROI's, great care was taken to include the entire lesion and exclude bleeding and calcification. Each ROI was scanned three times, and the average value was used as the final FA and ADC value.

Gleason score analysis. Gleason score analysis was used to evaluate the prognosis of patients with prostate cancer using samples from a prostate biopsy or surgery based on the microscopic appearance. A total score was calculated based on how cells looked under a microscope, with half the score based on the appearance of the most common cell morphology (scored 1-5) and the other half based on the appearance of the second most common cell morphology (scored 1-5). These two numbers were then combined to produce a total score for the cancer. Gleason scores ranged from 2-10, with higher numbers indicating higher aggression and poorer prognosis (6).

Statistical analysis. An IBM SPSS 19.0 (IBM Corp, Armonk, NY, USA) software package was used for data processing and statistical analysis. Pearson correlation analysis was conducted in order to determine whether there was a correlation of the FA and ADC values of PCa with the Gleason scores of the lesions. Measurement data are presented as the mean \pm standard deviation. $P < 0.05$ was determined to indicate statistically significant difference.

Results

Features of FA, ADC, DWI and DTT map of PCa at different disease grades. Among the 50 cases of PCa, 26 cases presented with Gleason scores of ≤ 6 , 13 cases presented with a Gleason score of 7 and 11 cases had Gleason scores of ≥ 8 ; these patients were grouped into low-, intermediate- and high-grade groups, respectively. The T2WI-FS image presented the clearest anatomical information, revealing that the lesion was confined to the outer peripheral area of the prostate in 8 cases, confined to the central gland area in 5 cases, located through the prostate capsule in 32 cases and simultaneously involved the peripheral and central gland region in 5 cases. In addition, 15 cases of lymph node and bone metastasis were observed. PCa lesions in the FA maps were presented as a mixed signal, a low signal in the ADC maps and a high signal in the DWI maps. According to the DTT maps, the PCa fiber bundle was interrupted in 6 cases of the high-grade group, but not interrupted in the low-grade and intermediate-grade groups. The characteristic features of the different groups according to the FA, ADC, DWI and DTT maps are presented in Table I and Figs. 1-3.

Association of FA and ADC values with the Gleason score in different groups. The FA and ADC values of the different groups are presented in Table II. FA values of the low-, intermediate- and high-grade groups were 0.284 ± 0.313 , 0.293 ± 0.347 and 0.369 ± 0.347 . Differences between the

Table I. Features of FA, ADC, DWI and DTT maps of prostate cancer at different grades of the disease.

Group	FA	ADC	DWI	DTT
Low grade	Hybrid high signal	Low signal	Slightly high signal	Fiber bundles in the cancer region were densely arranged and without interruption.
Intermediate grade	Hybrid high signal	Low signal	Medium high signal	Fibrous bundle arrangement disorder, sparse
High grade	Hybrid high signal	Low signal	High signal	Fiber bundle disruption and deletion in cancer foci

FA, fractional anisotropy; ADC, apparent diffusion coefficient; DWI, diffusion-weighted imaging; DTT, diffusion tensor tractography.

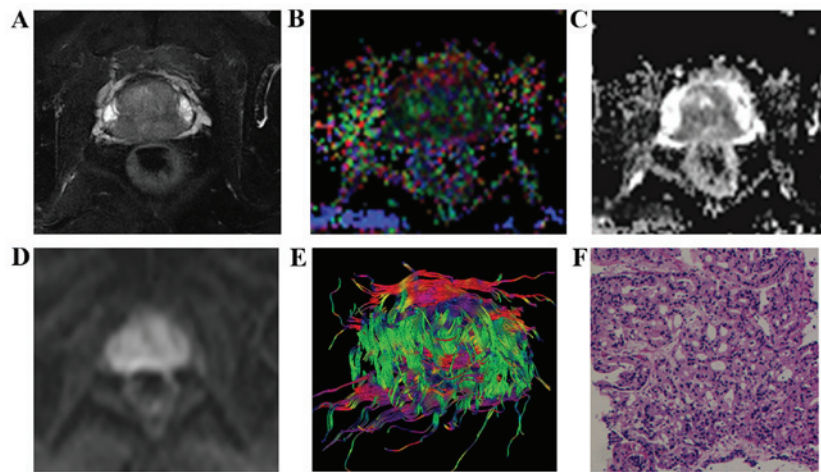


Figure 1. Characteristic signs and pathological comparison of T2WI-FS, FA, ADC, DWI and DTT maps in the low-grade group in a 65-year-old patient (prostate-specific antigen level, 27.33 ng/ml). (A) T2WI-FS indicated that the prostatic central gland zones and the rear part of the surrounding area exhibited a low signal. (B) FA map indicated lesions with mixed high signal (FA value, 0.269). (C) ADC map indicating lesions under homogeneous low signal (ADC value, 1.032×10^{-3} mm²/sec). (D) DWI revealed lesions with a slightly high signal. (E) DTT demonstrated that the fiber bundle was dense, orderly arranged and had no evident disruption. (F) Pathologic analysis indicated presence of prostate cancer (hematoxylin and eosin staining; magnification, x100; Gleason score, 3+3=6). T2WI, T2-weighted imaging; FA, fractional anisotropy; ADC, apparent diffusion coefficient; DWI, diffusion-weighted imaging; DTT, diffusion tensor tractography.

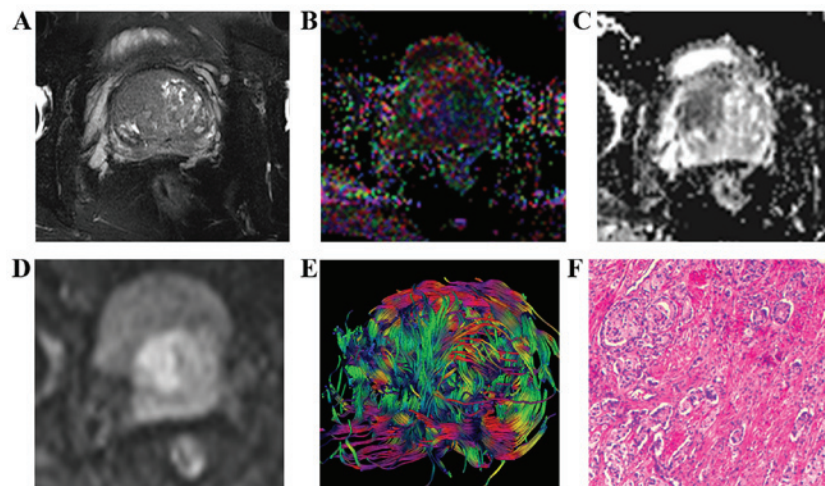


Figure 2. Characteristic signs and pathological comparison of T2WI-FS, FA, ADC, DWI, and DTT maps in the intermediate-grade group in a 78-year-old patient (prostate-specific antigen, 81.62 ng/ml). (A) T2WI-FS indicated that the prostatic central gland zones at the front right had a lower signal than benign prostatic hyperplasia. (B) FA map indicated a lesion area with mixed high signal (FA value, 0.295). (C) ADC map displays lesions under homogeneous low signal (ADC value, 0.868×10^{-3} mm²/sec). (D) DWI indicated lesions with a moderate to high signal. (E) DTT indicated lesion area fiber bundles arranged irregularly. (F) Pathological analysis demonstrating prostate cancer (hematoxylin and eosin; magnification, x100; Gleason score, 4+3=7). T2WI, T2-weighted imaging; FA, fractional anisotropy; ADC, apparent diffusion coefficient; DWI, diffusion-weighted imaging; DTT, diffusion tensor tractography.

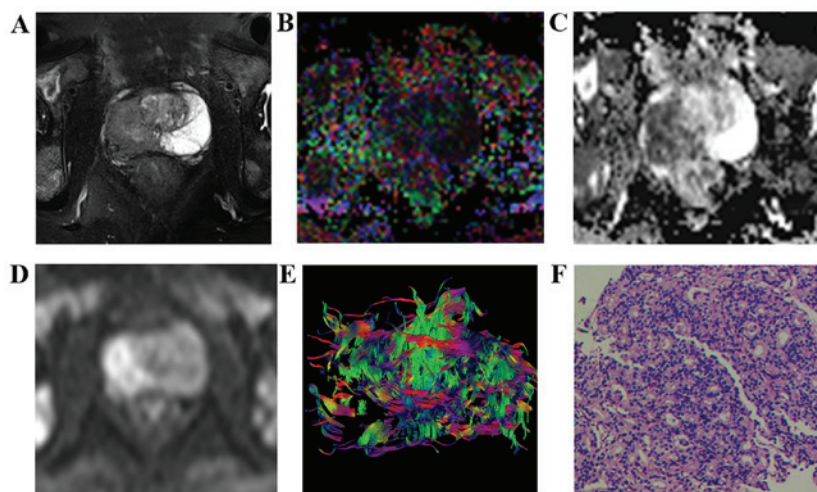


Figure 3. Characteristic signs and pathological comparison of T2WI-FS, FA, ADC, DWI, and DTT maps in the high-grade group in a 73-year-old patient (prostate-specific antigen, 70.59 ng/ml). (A) T2WI-FS indicated a tumor on the right side of the prostate peripheral zone with a lower signal compared with the contralateral, and bilateral acetabulum bone metastasis. (B) FA map indicated a lesion area with a mixed high signal (FA value, 0.338). (C) ADC map indicated lesions with a low signal (ADC value, $0.776 \times 10^{-3} \text{ mm}^2/\text{sec}$). (D) DWI indicated lesions with a high signal. (E) DTT map displays disorder, interruption and deletion in the cancer foci area fiber bundles. (F) Pathological analysis indicated prostate cancer (hematoxylin and eosin; magnification, $\times 100$; Gleason score, 4+5=9). T2WI, T2-weighted imaging; FA, fractional anisotropy; ADC, apparent diffusion coefficient; DWI, diffusion-weighted imaging; DTT, diffusion tensor tractography.

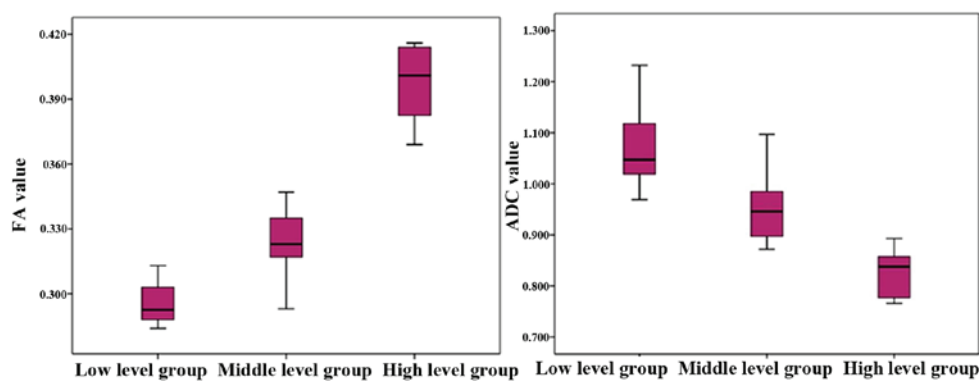


Figure 4. Correlation of FA and ADC values with the Gleason score of PCa. FA value was gradually increased, and was positively correlated with Gleason score. ADC value was gradually decreased, and the score was negatively correlated with the Gleason score. FA, fractional anisotropy; ADC, apparent diffusion coefficient; PCa, prostate cancer.

Table II. FA and ADC values of prostate cancer in the different groups ($\times 10^{-3} \text{ mm}^2/\text{sec}$).

Group	FA value	ADC value
Low grade	0.284 ± 0.313	1.070 ± 0.072
Intermediate grade	0.293 ± 0.347	0.961 ± 0.081
High grade	0.369 ± 0.347	0.821 ± 0.048
F-value	234.533	49.987
P-value	$<0.05^{a,b,c}$	$<0.05^{a,b,c}$

^aLow grade vs. intermediate grade. ^bLow grade vs. high grade. ^cIntermediate grade vs. high grade. FA, fractional anisotropy; ADC, apparent diffusion coefficient.

groups were statistically significant ($F=234.533$; $P<0.05$). In addition, the FA value was positively correlated with Gleason

classification ($r=0.884$; $P<0.05$), suggesting that the FA value increased with an increasing disease grade and Gleason score (Fig. 4).

ADC values of the low-, intermediate- and high-grade groups were $1.070 \pm 0.072 \times 10^{-3}$, $0.961 \pm 0.081 \times 10^{-3}$ and $0.821 \pm 0.048 \times 10^{-3}$, respectively, and the differences between the three groups were statistically significant ($F=49.987$; $P<0.05$); Furthermore, the ADC value was negatively correlated with the Gleason grading ($r=-0.810$; $P<0.05$), indicating that the ADC value decreased when the cancer grade increased (Fig. 4).

Discussion

DTI is a type of DWI based on a novel functional MRI technique, which accurately describes the diffusion path of water molecules in the three-dimensional space, and facilitates the quantitative evaluation, at the cellular and molecular levels, of the pathological and physiological changes occurring in

tissues (13,14). This technique is widely used for imaging in the central nervous system and skeletal muscle system (15,16); however, the use of DTI for the diagnosis, classification and evaluation of PCa remains unknown (17-19).

With the increase of Gleason score of the lesion, decreased differentiation of tumor cells is observed and tumors with a higher score have closely arranged cells (6). In the current study, PCa foci in the T2WI-FS images presented as low signal, whereas tumors in 15 cases from the low-grade group exhibited the phenomenon of a local high signal as the remnants of a few glandular structures mixed in with the low signal background. In the high-grade group, this phenomenon was not observed. FA maps revealed a mixed blue/green signal and there were no evident differences between the groups. ADC values and DWI are used to determine the grades of PCa foci (19). The findings of the present study suggested that, with an increase in the Gleason score of the tumor, the ADC value gradually decreased and the DWI map signal gradually increased. These changes may be due to the increasingly dense arrangement of cells in higher grade tumors, as well as the decrease of the extracellular space. In the DTT map, the fiber tracts in the low-grade and intermediate-grade groups demonstrated sparse and irregular distribution, with no marked disruption, while 6 cases in the high-grade group presented with marked disruption of the fiber bundle. Thus, it can be inferred that the low and intermediate grades of PCa exhibit low aggression and the high grade of PCa may invade adjacent tissue. Takayama *et al* (20) observed that the fiber bundles of PCa were deformed but with no evident disruption.

Gleason score serves an important role in predicting the extent of tumor invasion, lymph node and distant metastasis and patient outcomes (8). Currently, clinical Gleason scoring is performed in PCa specimens obtained by surgical resection or biopsy. Furthermore, the correlation between DTI and Gleason scores has been explored by measuring FA and ADC values, which may be beneficial in predicting the malignant degree of the tumor (20).

Previous study by Woodfield *et al* (21) revealed that there was a significant negative correlation of ADC value with Gleason score in PCa; namely with increasing Gleason score, ADC values gradually decreased. In addition, Li *et al* (22) reported that for PCa Gleason scores $\leq 3+3$, $3+4$, $4+3$ and $\geq 4+4$, ADC values were $1.11 \pm 0.16 \times 10^{-3}$, $0.98 \pm 0.14 \times 10^{-3}$, $0.91 \pm 0.13 \times 10^{-3}$ and $0.84 \pm 0.131 \times 10^{-3}$ mm²/sec, respectively, indicating a gradual reduction. The results of the present study were consistent with these aforementioned findings. So far, few studies have investigated the correlation between FA value of PCa and Gleason score. The results of Li *et al* (22) for Gleason scores of PCa of $3+3$, $3+4$, $4+3$ and $4+4$ indicated FA values of 0.26 ± 0.04 , 0.29 ± 0.03 , 0.30 ± 0.03 and 0.33 ± 0.04 , respectively; thus, FA values were found to be positively associated with Gleason scores. In addition, Gong *et al* (23) and Wang *et al* (24) indicated that FA values and Gleason scores were negatively correlated, suggesting that an increase in Gleason scores would cause a gradual reduction in FA value. The main factors affecting the FA values are as follows: i) Following an increase in Gleason scores, the proliferation of mesenchymal structure of fibers and more closely arranged cells are observed, resulting in higher FA values; and ii) following an increase in Gleason score, the cell carcinoma is poorly differentiated, atypia increases and

erosion of the fibrous tissue structure is enhanced, resulting in fiber breakage, as well as disorganized and restricted water diffusion, thus leading to decreased FA values. The aforementioned studies (23,24) demonstrated that the second factor served a leading role, thus reducing the FA value. However, the results of the present study were consistent with those from Li *et al* (22). We hypothesize that the first factor affecting the FA value had a greater impact; the freedom of movement of water molecules was restricted and although prostate inherent normal fiber bundles were destroyed, this led to more freedom of movement of water molecules, but very little impact, therefore, higher FA values were observed in patients with higher Gleason grades. Although studies have reported that the ADC and FA values of PCa tumors are correlated with the Gleason grade, conflicting results exist. The use of ADC and FA values to predict the malignancy degree of the tumor requires further investigation in large-scale studies (22-24).

The present study had some limitations. The application of DTT for the diagnosis of PCa was conducted at different research institutions with the use of equipment produced by different companies and different scanning parameters, which may affect the consistency of the results. Therefore, it is critical that the method used for DTT for diagnosis is standardized. DTT only provides visual information; quantitative measurements and statistical analyses are not available. Thus, it is not possible to accurately judge the reasons for fiber bundle damage, such as direct tumor invasion, tumor compression or vasogenic edema. DTT maps mainly present the interstitial structure, not the glandular and glandular tube structure, resulting in limitations in the use of this technique.

In conclusion, the present study combined quantitative parameter values (FA and ADC values) and parametric diagrams (FA, ADC, DWI and DTT maps), which fully revealed the correlation of FA and ADC values with the Gleason score of PCa. These values may be used to assess PCa invasiveness and prognosis, allowing the development of a clinical individualized treatment plan.

Acknowledgements

The present study was supported by grants from the Scientific Research Project of Jiangsu Provincial Commission of Health (grant no. H201262), the Suzhou Science and Technology Development Plan (grant no. SS201534) and Clinical Special Disease Diagnosis and Treatment Technology in Suzhou (grant no. LCZX201406).

References

1. Siegel RL, Miller KD and Jemal A: Cancer statistics, 2017, *CA Cancer J Clin* 67: 7-30, 2017.
2. Wang YJ, Fu ZX, Wang J, *et al*: Incidence and mortality of prostate cancer among residents in Luwan district of Shanghai, 2004-2011. *Chin Cancer* 26: 438-441, 2017.
3. Heidenreich A, Bastian PJ, Bellmunt J, Bolla M, Joniau S, van der Kwast T, Mason M, Matveev V, Wiegel T, Zattoni F, *et al*: EAU guidelines on prostate cancer. Part 1: Screening, diagnosis, and local treatment with curative intent-update 2013. *Eur Urol* 65: 124-137, 2014.
4. Chinese Journal of Radiology in the diagnosis of prostatic diseases, Chinese Journal of Radiology, editorial board of the Chinese Journal of radiology: MR examination and diagnosis of prostate cancer. *Chin J Radiol* 48: 531-534, 2014.

5. Bazot M, Bharwani N, Huchon C, Kinkel K, Cunha TM, Guerra A, Manganaro L, Buñesch L, Kido A, Togashi K, *et al*: European society of urogenital radiology (ESUR) guidelines: MR imaging of pelvic endometriosis. *Eur Radiol* 27: 2765-2775, 2017.
6. Liao LH, Wang SH and Shen JH: The formation, development and application of Gleason grading system for prostate cancer. *J Diag Pathol* 19: 309-312, 2012.
7. Kagebayashi Y, Nakai Y, Matsumoto Y, Samma S, Miyasaka T and Nakagawa H: Utility of diffusion-weighted magnetic resonance imaging and apparent diffusion coefficient in detection of prostate cancer and prediction of pathological Gleason score. *Hinyokika Kyo* 58: 405-408, 2012 (In Japanese).
8. Wu CJ, Wang Q, Li H, Wang XN, Liu XS, Shi HB and Zhang YD: DWI-associated entire-tumor histogram analysis for the differentiation of low-grade prostate cancer from intermediate-high-grade prostate cancer. *Abdom Imag* 40: 3214-3221, 2015.
9. Caivano R, Rabasco P, Lotumolo A, Cirillo P, D'Antuono F, Zandolino A, Villonio A, Macarini L, Salvatore M and Cammarota A: Comparison between Gleason score and apparent diffusion coefficient obtained from diffusion-weighted imaging of prostate cancer patients. *Cancer Invest* 31: 625-629, 2013.
10. Bammer R, Acar B and Moseley ME: In vivo MR tractography using diffusion imaging. *Eur J Radiol* 45: 223-234, 2003.
11. Sinha S and Sinha U: In vivo diffusion tensor imaging of the human prostate. *Magn Reson Med* 52: 530-537, 2004.
12. Gibbs P, Pickles MD and Turnbull LW: Diffusion imaging of the prostate at 3.0 tesla. *Invest Radiol* 41: 185-188, 2006.
13. Basser PJ, Mattiello J and LeBihan D: MR diffusion tensor spectroscopy and imaging. *Biophys J* 66: 259-267, 1994.
14. Le Bihan D, Mangin JF, Poupon C, Clark CA, Pappata S, Molko N and Chabriat H: Diffusion tensor imaging: Concepts and applications. *J Magn Reson Imaging* 13: 534-546, 2001.
15. Wang S, Kim SJ, Poptani H, Woo JH, Mohan S, Jin R, Voluck MR, O'Rourke DM, Wolf RL, Melhem ER and Kim S: Diagnostic utility of diffusion tensor imaging in differentiating glioblastomas from brain metastases. *AJNR Am J Neuroradiol* 35: 928-934, 2014.
16. Schenk P, Siebert T, Hiepe P, Güllmar D, Reichenbach JR, Wick C, Blickhan R and Böl M: Determination of three-dimensional muscle architectures: Validation of the DTI-based fiber tractography method by manual digitization. *J Anat* 223: 61-68, 2013.
17. Gürses B, Tasdelen N, Yencilek F, Kılıckesmez NO, Alp T, Fırat Z, Albayrak MS, Uluğ AM and Gürmen AN: Diagnostic utility of DTI in prostate cancer. *Eur J Radiol* 79: 172-176, 2011.
18. Gürses B, Kabakci N, Kovanlikaya A, Fırat Z, Bayram A, Uluğ AM and Kovanlikaya I: Diffusion tensor imaging of the normal prostate at 3 Tesla. *Eur Radiol* 18: 716-721, 2008.
19. Xia G, Gong H, Zeng X, *et al*: MR diffusion tensor imaging in the diagnosis of prostate cancer. *Chin J Radiol* 46: 526-528, 2012.
20. Takayama Y, Kishimoto R, Hanaoka S, Nonaka H, Kandatsu S, Tsuji H, Tsujii H, Ikehira H and Obata T: ADC value and diffusion tensor imaging of prostate cancer: Changes in carbon-ion radiotherapy. *J Magn Resonance Imag* 27: 1331-1335, 2008.
21. Woodfield CA, Tung GA, Grand DJ, Pezzullo JA, Machan JT and Renzulli JF II: Diffusion-weighted MRI of peripheral zone prostate cancer: Comparison of tumor apparent diffusion coefficient with Gleason score and percentage of tumor on core biopsy. *AJR Am J Roentgenol* 194: W316-W322, 2010.
22. Li L, Margolis DJ, Deng M, Cai J, Yuan L, Feng Z, Min X, Hu Z, Hu D, Liu J and Wang L: Correlation of gleason scores with magnetic resonance diffusion tensor imaging in peripheral zone prostate cancer. *J Magn Reson Imaging* 42: 460-467, 2015.
23. Gong T, Yuan SH, Li LL, *et al*: Study on the correlation between prostate cancer DTI parameters and Gleason score. *Med Imag J* 24: 574-577, 2014.
24. Wang Q, Gong T and Wang XZ: 3.0T diffusion tensor imaging in the evaluation of prostate cancer Gleason score value. *J Clin Radiol* 34: 581-585, 2015.